frontiers in Materials

ORIGINAL RESEARCH
published: 28 July 2020
doi: 10.3389/fmats.2020.00205

Roles of Size, Shape, Amount, and Functionalization of Nanoparticles of Titania in Controlling the Tribo-Performance of UHMWPE Composites

*Meghashree Padhan, Gourab Paul and Jayashree Bijwe**

Centre for Automotive Research and Tribology (Formerly ITMMEC), Indian Institute of Technology Delhi, Hauz Khas, India

The present research is based on development and performance evaluation of ultra-high molecular weight polyethylene composites with Titania particles in various amounts and of two sizes, including nano-size. It also included functionalization of nanoparticles (NPs) with a siloxane group to enhance adhesion with the matrix, which would help to reduce wear. Thus, the work had several objectives such as to investigate the effect of size (nano vs. micro) and determine the amount that delivers the best performance from among a series of composites with different Titania particle amounts [0–8% in the case of microcomposites (MCs) and 0–4% in the case of nanocomposites (NCs)]. It was also of interest to examine the effect of siloxane-functionalization of NPs [since they performed significantly better than microparticles (MPs)] on the performance of NCs. It was observed that for adhesive and erosive wear modes, both types of particles (MPs and NPs) proved detrimental in spite of the enhanced hardness of the composites, essentially because of the irregular shape of particles, which altered the wear mechanisms adversely. Nanoparticles proved less detrimental, while F-NPs (functionalized NPs) proved marginally detrimental. In abrasive wear mode, both proved beneficial, NPs being more effective than MPs, and F-NPs proved the best. The studies revealed how the shape of particles influences the performance of composites in various wear modes.

Keywords: UHMWPE, TiO_2, siloxane treatment, abrasive and adhesive wear, erosion

OPEN ACCESS

Edited by:
Patricia Krawczak, IMT Lille Douai, France

Reviewed by:
Sergey Panin, Institute of Strength Physics and Materials Science (ISPMS SB RAS), Russia
Abdul Samad Mohammed, King Fahd University of Petroleum and Minerals, Saudi Arabia
Z. Peng, University of New South Wales, Australia

***Correspondence:**
Jayashree Bijwe
jbijwe@gmail.com

Specialty section:
This article was submitted to Polymeric and Composite Materials, a section of the journal Frontiers in Materials

Received: *27 March 2020*
Accepted: *04 June 2020*
Published: *28 July 2020*

Citation:
Padhan M, Paul G and Bijwe J (2020) Roles of Size, Shape, Amount, and Functionalization of Nanoparticles of Titania in Controlling the Tribo-Performance of UHMWPE Composites. Front. Mater. 7:205. doi: 10.3389/fmats.2020.00205

INTRODUCTION

Ultra-high molecular weight polyethylene (UHMWPE) and its composites are being widely used for applications like producing bottles for runners, chain guides, and lining for coal chutes and also as bearing material in agricultural and mining equipment due to their excellent wear resistance coupled with their low coefficient of friction (μ), along with ease of availability and cost viability. Moreover, UHMWPE is extensively used in a composite form as a bearing material for implants (joint replacements for the hip, knee, and ankle) (Wang et al., 2007; Ge et al., 2009; Holland et al., 2018; Gao et al., 2019; Ortiz-Hernández et al., 2019). It shows excellent wear resistance (W_R) in almost all wear modes (Lee, 1985) along with ultra-low μ, high specific strength and modulus,

toughness, very good dampening capability, excellent resistance to chemicals, etc. Efforts are being made to maximize its W_R, especially by selecting biocompatible fillers like titania, zirconia, etc., and their use as nanoparticles (NPs). The final performance of nanocomposites (NCs) depends on the type of matrix and NPs, their amount, size, shape, filler-matrix adhesion, etc. A lot has been reported on the exploration of various types and amounts of hard NPs (non-bio-compatible) to enhance the W_R of UHMWPE (Chang et al., 2013; Xu and Tangpong, 2013; Chukov et al., 2014; Sharma et al., 2015, 2016; Kumar et al., 2017).

Xu and Tangpong (2013) presented the current trends of research in the tribology of polyethylene-based NCs along with the type of nano-fillers used and the processing approaches. It was stated that agglomeration takes place in a higher concentration of NPs, resulting in deterioration of wear performance.

Few papers have reported on the surface treatment/functionalization of fillers/fibers to improve the performance with UHMWPE. Chukov et al. (2014) studied the effect of nitric acid treatment of carbon fibers leading to enhanced adhesion with the matrix and hence improved mechanical properties. Tribo-properties, however, were not studied. Chang et al. (2011) reported improvement in mechanical and antibacterial properties of UHMWPE due to reinforcement with silane-treated zinc oxide particles (<1 μm) compared to untreated ones. However, no tribo-studies were reported. Kandeva et al. (2018) reported the effect of multi-walled carbon nano-tubes (CNTs) untreated and modified with electro-less nickel plating. Tribo-studies were done in a thumb disk tribo-setup in abrasive wear mode. Modified CNTs showed higher W_R as compared to the unmodified ones.

A lot of patents are available on the applications of UHMWPE in composite form for the biomedical area (Senatov et al., 2014; Coker, 2019; Gopanna et al., 2019; Salari et al., 2019; Saravanan and Devaraju, 2019; Duan et al., 2020)[1,2]. Several researchers have recommended their composites for such applications. Duan et al. (2020) studied the thermal stability and mechanical properties of irradiation-cross-linked graphene oxide/UHMWPE composites with vitamin E. The crystallinity, thermal stability, hardness and scratch resistance, and oxidation resistance of the composites improved as compared to UHMWPE, but at the cost of a slight deterioration in mechanical properties. The fatigue strength, compressive and tensile properties, and wear resistance of the modified composites were not investigated. These composites were claimed to have bright application prospects in the field of artificial joint replacement owing to some further investigations. Senatov et al. (2020) prepared a novel biomimetic highly porous UHMWPE/Hydroxyapatite (HA) (40 wt.%) scaffold for reconstructive surgery with a porosity of 85 vol.%. This biocompatible highly porous UHMWPE/HA scaffold, used separately or in combination with proteins for the reconstruction of non-load bearing parts of bones, was reported to solve the problems associated with differences between implant architecture and trabecular bone, low osteointegration, and bio-inertness. Saravanan and Devaraju (2019) tribo-investigated an γ-irradiated composite of UHMWPE (80 wt.%), alumina (3 wt.%), HA (5 wt.%), and Chitosan (12 wt.%) and reported a 1.3 times increase in tribo-performance due to irradiation. The composites were targeted at biomedical applications. Salari et al. (2019) studied the effect of nano-zirconia (2, 6, and 10 wt.%) in HP (10 wt.%)-reinforced UHMWPE composites and reported significantly improved mechanical properties and wear resistance in comparison with HAp alone and furthermore eliminated the concern of wear debris and adverse biological responses caused by osteolysis. Zirconia also demonstrated exceptional biological responses in the presence of MG-63 osteoblast cell cultures, showing no cytotoxicity and high alkaline phosphatase activity along with fully spread osteo-cells. Hence, the authors claimed it as a promising material for overcoming the shortcomings of the conventionally used UHMWPE as an implant liner. Gopanna et al. (2019), in their overview of polyethylene and polypropylene composites for biomedical applications, suggested that UHMWPE composites reinforced with NPs, nanotubes, and nanofibers should be used in orthopedic bearing applications. Chemically cross-linked UHMWPE filled with particles of Al, Cu Fe, and reinforced with quartz particles of micron size have been developed for orthopedic applications.

Titanium dioxide (TiO_2)/Titania is a hard filler with excellent resistance to UV and chemicals and is also known for bio-compatibility (Hashimoto et al., 2003; Gutwein and Webster, 2004; Lei et al., 2010; Sabetrasekh et al., 2011; You et al., 2014; Celebi Efe et al., 2019). **Supplementary Appendix A** gives details on various available papers on UHMWPE-TiO_2 composites with special reference to NPs and their functionalization (Hu et al., 2016; Celebi Efe et al., 2017; Yu et al., 2017). It seems that only two papers dealt with NPs, and these did not look into tribo-effects (Ortiz-Hernández et al., 2019; Duan et al., 2020). Some papers (Duan et al., 2020; see footnote 1) reported on the functionalization of microparticles (MPs) but not in detail by reporting tribology. Thus, it was concluded that in-depth studies of UHMWPE-Titania composites (MCs and NCs) are required with the following aims, since they are not met in the literature.

- Assess the potential of NPs vs. MPs to improve the tribo-performance in various wear modes.
- Determine the influence of increasing amounts of NPs (realistic amount) and MPs as a means to find the optimum amount for the best W_R value.
- Determine the effect of functionalization of NPs with siloxane treatment on tribo-performance in various wear modes.

With these aims in view, three series of UHMWPE-Titania composites – the first with MPs (0–8%), the second with NPs (0–4%), and the third with functionalized NPs (0–4%) – were developed and characterized for tribo-performance in three wear modes, viz., adhesive, abrasive, and erosive, and the findings are presented in subsequent sections.

[1]https://ryortho.com/breaking/b-one-total-hip-cleared-by-fda/

[2]https://www.materialsforengineering.co.uk/engineering-materials-news/researchers-create-radiopaque-polyethylene-for-the-visualisation-of-medical-implants/110699/

MATERIALS AND METHODS

Materials and Characterization of Particles

Ultra-high molecular weight polyethylene was procured in a particulate form (≈40 μm) from Bhilwara Polymers Ltd., Rajasthan; details of its properties are given in **Table 1**.

Titania (TiO_2) nano (10–25 nm)- and MPs (30–40 μm) were procured from Nano Shell LLC United States. The size was verified with SEM (scanning electron micrograph; Zeiss EVO MA 10) and TEM (transmission electron micrograph; JEOL JEM-1400 Plus), as shown in **Figures 1a,b**, respectively. It seems that MPs were of highly irregular shape and NPs were of 40–50 nm size and also of irregular shape. **Figure 1-II** shows the SEM and EDAX micrographs of selected specimens (V_{8M}, V_{2M},V_{2N}, and F_{2N}) cut to expose the inside transverse section. This was done to determine whether particles are uniformly distributed in the bulk of the composites. Dot maps of Ti represent the distribution of TiO_2 particles irrespective of size. For F_{2N}, additional dot mapping was done for Si element to ensure the presence of siloxane treatment on the particles.

The XRD-X-ray diffraction spectrum (Phillips XPERT-PRO) of NPs was collected to verify the size, and the data are shown in **Figure 1-III**.

The crystallite size of NPs was determined using the Debye–Scherrer method using the following equation (Holzwarth and Gibson, 2011).

$$t = \frac{0.9\lambda}{B\ \cos\theta} \tag{1}$$

where λ is the characteristic wavelength, B is the full width at half maximum, and θ is the midpoint of the peak. The XRD shows coherent diffraction regions that imply the size of the crystallites for the respective diffraction peak. A particle may be made up of several different crystallites or just one crystallite. Sometimes, it also corresponds to the size of the grain s of an analyte sample, or the thickness of a polycrystalline thin film or bulk material. **Supplementary Appendix A** collects the data from XRD.

Overall, it was confirmed that the approximate crystallite size of the particles was in the range of 23–27 nm as observed from the first three peaks.

Experimental Work

Surface Modification of Nanoparticles

For siloxane treatment of NPs, Amino propyl tri-ethoxy silane (APTES) was used (procured from Alpha Aesar). The basic aim of the surface modification of TiO_2 NPs was to impart siloxane functional groups to the surface of particles, which would bridge with matrix, resulting in enhanced filler-matrix adhesion in the composites. It was anticipated that this might lead to improved tribological properties (less wear). Surface modification of TiO_2 with APTES was done as per a reported process as shown in **Figure 2** (Chukov et al., 2014) using reflux reaction and mechanical stirring, with xylene as a medium and at 50°C in a silicon oil bath for varying durations, as shown by **Table 2**.

The particles were washed using xylene, followed by ethanol two times, and finally with acetone. They were then filtered using a REMI PR-24 centrifuge followed by drying under vacuum. Fourier Transform Infrared (FTIR) Spectroscopy was done in attenuated transmission reflectance (ATR) mode in a Nicolet IS 50 for confirmation of the presence of siloxane treatment on the particles as well as for optimization of the time duration of the treatment. The analysis was performed for an iteration of 32 scans for accuracy of results (**Table 2**).

TABLE 1 | Properties of UHMWPE as per the supplier's data.

Property	Value
Density (g/cm^3)	0.93
Tensile strength at yield (MPa)	21
Tensile strength at break (MPa)	48
Hardness, Shore D	62–66
Crystalline melting range, powder, °C	138–142

Development of UHMWPE Composites

Uniform dispersion of micro- and nano-TiO_2 particles is extremely important. De-agglomeration of NPs was performed using a Crome Tech Probe Sonicator (UP-800 ultrasonic processor). An accurately weighed amount of NPs was added to double-distilled water in installments, followed by sonication for two minutes (pulse time 2 s, and pulse off for 5 s, at 800 W) after each installment, the total time of sonication being 30 min. A weighed amount of UHMWPE was then added to this suspension in installments followed by sonication to achieve homogeneous dispersion of NPs and UHMWPE in double-distilled water. A similar procedure was employed in the case of microcomposites (MCs) to maintain uniformity.

Nano- and microcomposites of UHMWPE with TiO_2 were developed by using a compression molding technique under temperature (180°C) and pressure (12–15 bar). The mold was fast cooled using water cooling. The compositions of the composites developed are shown in **Table 3**.

Characterization of Composites

Density

The density of the composites was measured to characterize them, since density is the first basic property. It also helped to gain an overall view of the void content in the composites and also to calculate the specific wear rate.

(a) Density was measured by the standard Archimedes principle following ASTM D792 using a Mettler Toledo weighing balance as per Eq (2). Acetone was used as the liquid, having a density of 0.79 g/cm^3 at 20°C.

$$\rho = \left(\rho_{\text{liquid}} \times W_{\text{air}}\right) / \left(W_{\text{air}} - W_{\text{liquid}}\right) \tag{2}$$

where ρ is the density of the composite, ρ_{liquid} is the density of the liquid used, and W_{air} and W_{liquid} are the weights of the composite in air and liquid.

The rule of mixtures was used to calculate the theoretical density of the composites using the following equation:

$$\rho_t = 1/\left(W_f/\rho_f + W_m/\rho_m\right) \tag{3}$$

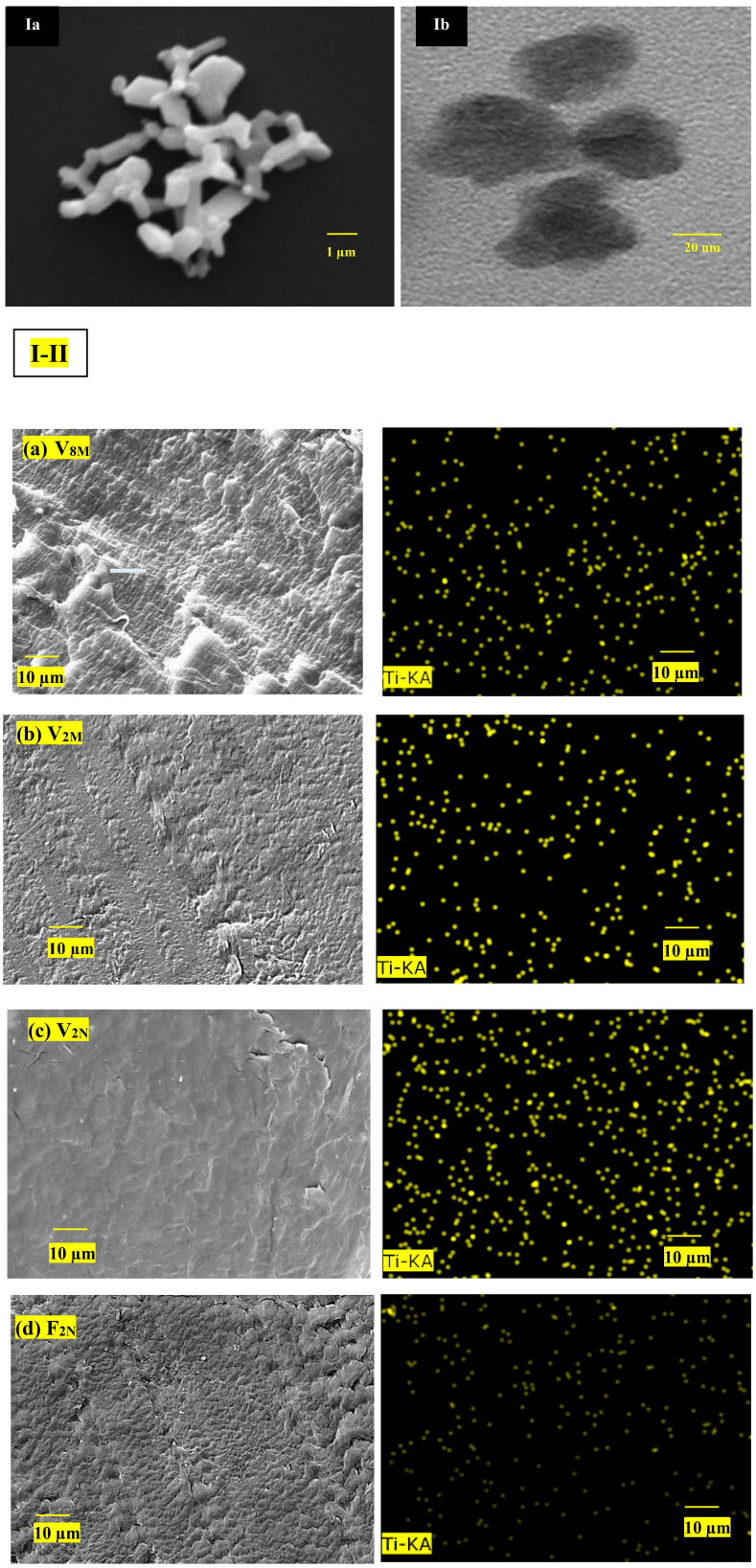

FIGURE 1 | Continued

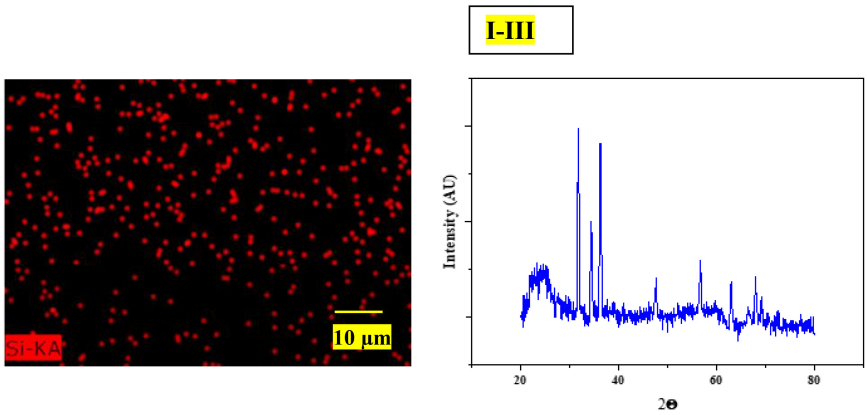

FIGURE 1 | Micrographs of TiO_2 particles; **(1a)** SEM of microparticles and **(1b)** TEM of nanoparticles; 1-II – SEM and EDAX micrographs of representative composites showing uniform distribution of filler particles; 1-III – X-ray diffraction pattern for nano-TiO_2 particles.

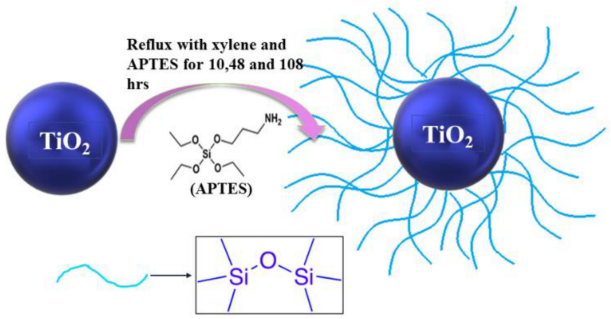

FIGURE 2 | Schematic of treatment of TiO_2 NPs with APTES.

TABLE 2 | Treatment of NPs of TiO_2 (1.5 g) with APTES (1.5 ml) in xylene as a medium (50 ml) at 50°C for various durations and the chemical changes confirmed from FTIR studies.

Treatment	Heating time (h)	Observation
Scheme 1	10	No change
Scheme 2	48	Low-intensity peak of –Si–O–; –O–Ti–O- peak
Scheme 3	108	Sharp and intense –Si–O– peak; –Ti–O–Si– peak

where ρ_m and ρ_f are the theoretical density of the matrix (UHMWPE; 0.93 g/cc) and the filler (Ti; 3.9 g/cc), respectively. W_m and W_f are the respective weight fractions.

(b) Void content.

The void content of the composites was calculated from the following equation:

$$Void\ content\ (\%) = \frac{\rho_{th} - \rho_c}{\rho_{th}} \times 100 \quad (4)$$

where ρ_{th} and ρ_c are the calculated and theoretical densities of the composite as obtained using Eqs 2 and 3.

Vickers Micro-Hardness

TiO_2, being a ceramic material, has an entirely different set of properties, especially hardness, as compared to the softer polymeric phase. It was necessary to examine the extent of its implications for the hardness properties of UHMWPE since hardness is generally well-correlated with abrasive wear performance. The Vickers hardness of the composites was measured as per ASTM E92-82. The composites were polished against 1000 grade *SiC* abrasive paper. A square-based pyramidal diamond indenter with included face angles of 136° was penetrated into the material with a force of 20 N. The Vickers hardness number (HV) is related to the applied force and surface area of the resultant permanent impression according to the following equation:

$$HV = 1.8544 \times \frac{F}{d^2} \quad (5)$$

where F is the force applied and d is the mean diagonal diameter of the impression.

Scanning Electron Microscopy and Energy Dispersive X-ray Spectroscopy

Microscopic worn surface analysis, generally performed with SEM, furnishes a lot of information about the surface topography, damage, and deterioration level of matrix and filler-matrix adhesion, dominating wear mechanisms, etc. An SEM (Zeiss, EVO-MA 10) was used to study the worn surfaces of the composites. The samples were gold-coated to make them conducting using a Cressington Sputter Coater 108.

Wettability Analysis

The wettability of matrix and its composites differ based on the type and amount of filler and also filler-matrix bonding. Generally, this property is evaluated by water drop (the sessile drop method), and reduction in the contact angle is an indication of a higher ceramic content and higher filler-matrix adhesion. The contact angle on the surface of selected composites (V, V_{2N}, and F_{2N}) was measured using a KRUSS GmbH DSA

TABLE 3 | Composition and coding of composites.

(A) Micro-Series with untreated Titania microparticles						
Micro-Series	**TiO_2 (wt.%) Untreated**	**0**	**2**	**4**	**6**	**8**
Codes		**V_0**	**V_{2M}**	**V_{4M}**	**V_{6M}**	**V_{8M}**
Theoretical density (g/cc)		0.930	0.985	1.0416	1.09	1.153
Practical density (g/cc)		0.930	0.952	0.967	0.972	0.996
Void content (%)		0	3.3	7	10	13.61
Vickers Hardness (MPa)		6.621	6.968	7.05	7.15	7.26
(B) Nano-Series with untreated Titania nanoparticles						
Nano-Series	**TiO_2 (wt.%) Untreated**	**0**	**1**	**2**	**3**	**4**
Codes		**V_0**	**V_{1N}**	**V_{2N}**	**V_{3N}**	**V_{4N}**
Theoretical density (g/cc)		0.930	0.965	0.98	1.01	1.04
Practical density (g/cc)		0.930	0.963	0.967	0.971	0.975
Void content (%)		0	0.2	1.32	3.8	6.25
Vickers Hardness (MPa)		6.621	7.56	8.14	9.42	9.876
(C) Nano-Series with treated Titania nanoparticles						
Nano-Series with treated particles	**TiO_2 (wt.%) Treated**	**0**	**1**	**2**	**3**	**4**
Codes		**V_0**	**F_{1N}**	**F_{2N}**	**F_{3N}**	**F_{4N}**
Theoretical density (g/cc)		0.93	0.963	0.967	0.971	0.975
Practical density (g/cc)		0.93	0.964	0.969	0.974	0.979
Void content (%)		0	0	0	0	0
Vickers Hardness (MPa)		6.621	7.85	8.21	9.45	9.88

25S. The surfaces were cleaned by sonication in acetone prior to the experiment. A 2-μl drop of deionized water was placed on the surface. The contact angles at different positions were averaged out.

Roughness Measurement

The surface roughness of composites is a tool with which to quantify the texture/topography of the worn surfaces and is correlated with the extent of wear-damage. The surface roughness of the wear track was measured using a Micro-Xam 100 stylus-type profiler manufactured by KLA-Tencor. The roughness data are the average of three points across various areas on the wear track.

Tribological Characterization

Tribological studies were performed to evaluate the performance of the developed composites in various wear modes, viz., adhesive (sliding against a smooth counterface), abrasive (sliding against a rougher and harder counterface), and erosive (impingement of harder abrasive particles at different angles) wear modes.

Adhesive wear

The adhesive wear performance of the composites was evaluated on a UMT-3MT Tribometer supplied by CETR/Bruker, United States. During initial studies on a pin (polymeric) on metallic disk configuration, hardly any loss in weight of the pin was observed, even after running the test for 4 h, because of the exceptionally high wear resistance of UHMWPE. Hence, a ball (AISI 52100 steel – R_a – ≈50 nm) on disk (polymer) configuration was selected to increase the pressure and also the dissipativity of frictional heat, since point contact has these advantages. A 10-mm ball rotated on a polymeric disk in a wear track, as shown in **Figure 3A**. The tests were conducted under 200 N (P 73 MPa), keeping other parameters such as v (0.15 m/s), rpm (100), sliding distance (4220 m), and duration (4 h) constant.

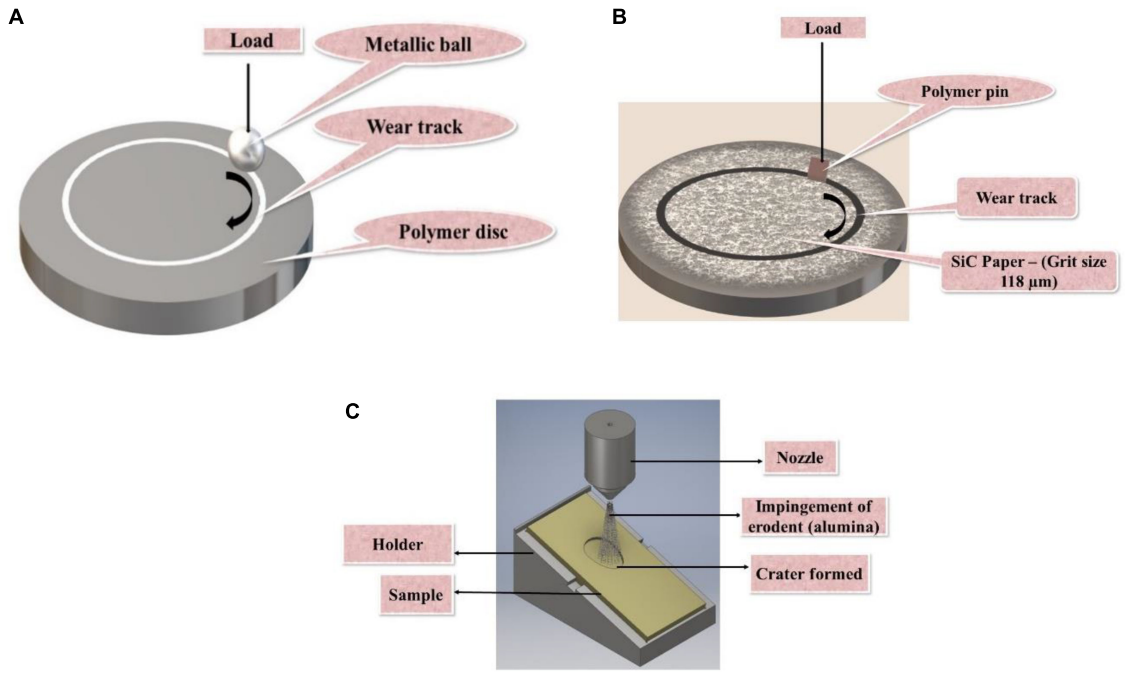

FIGURE 3 | Configurations in **(A)** adhesive wear, **(B)** abrasive wear, and **(C)** erosive wear.

The specific wear of the disk (K_0) (m^3/Nm) was calculated as follows.

$$K_0 = \frac{\Delta W}{\rho \times L \times D} \left(\mathrm{m}^3/\mathrm{Nm}\right) \quad (6)$$

where ΔW – weight loss in kg; ρ – density in kg/cm^3, L – load in N; D – sliding distance completed in 4 h in meters.

The maximum Hertzian Pressure (P) was calculated as

$$P = \frac{F}{\pi a^2} \quad (7)$$

where F is the applied load (N) and a is the radius of the contact area (mm), calculated as

$$a = \left(\frac{3Fr}{4E^*}\right)^{1/3} \quad (8)$$

where r is the radius of the steel ball and E^* is the calculated modulus at contact.

Abrasive wear

Abrasive wear studies were conducted in the UMT-3MT Tribometer supplied by CETR/Brucker, United States in a pin on disk (POD) configuration (**Figure 3B**). Silicon carbide (*SiC*) abrasive paper of 1000 grade was used to achieve a uniform contact, while for testing purposes, 120 grade (118 μm grit size) was used for a single pass rotary motion. A 10-mm × 10-mm × 4-mm polymer pin was abraded at a constant speed of 0.025 m/s. The sliding distance of 1 m was achieved by changing four papers and was kept constant. In each experiment, all parameters except load were kept constant. Load was selected as a variable parameter and was varied between 25, 50, 75, and 100 N. After completion of the experiment, the pin was cleaned ultrasonically in acetone, dried, and weighed. The specific wear rate was calculated from the recorded weight loss using Eq. 6.

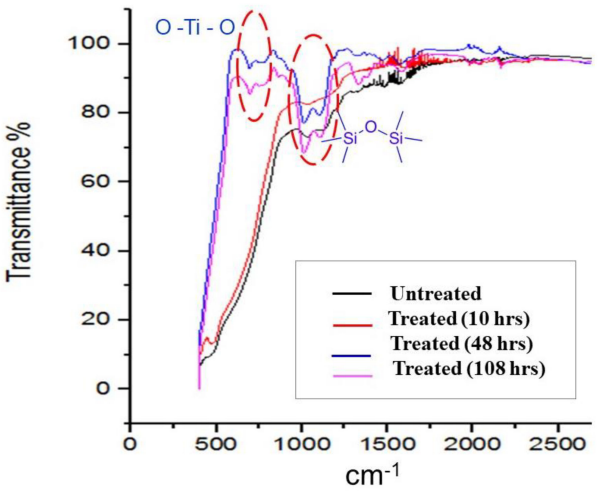

FIGURE 4 | FTIR analysis of siloxane-treated particles for varying treatment durations.

Erosive wear

The erosive wear tests on the UHMWPE composites were carried out on a TR-471-400 air jet erosion tester (Ducom Instruments Ltd., Bangalore). Ultra-high molecular weight polyethylene,

being a ductile material, shows high erosion at lower angles (Hutchings, 1992), and hence 15° and 30° were the two angles chosen for the studies. Alumina particles 60 μm in size were selected as the erodent, and the discharge rate was kept at 4 g/min and the velocity at 58 m/s using a 3-mm diameter Tungsten Carbide nozzle (**Figure 3C**). The tests were performed at 25°C, and the total mass of erodent was 240 g. Amount of wear was quantified by erosion (E), which was calculated by Eq. 9 (Chahar and Pun, 2018).

$$E = \frac{\text{Weight loss}}{\text{Mass of Erodent}}\ \text{g/g} \tag{9}$$

RESULTS AND DISCUSSION

Characterization Studies

FTIR Studies

The FTIR spectra for TiO_2 particles (treated and untreated) are shown in **Figure 4**.

The broad band observed in the region 600–400 cm^{-1} corresponded to the –Ti–O–Ti– stretching vibration peak (Ukaji et al., 2007; Mallakpour and Nikkhoo, 2013). In-plane O–H bending vibration corresponds to peaks at 1399 and 1630 cm^{-1} on the surface of TiO_2. The band at 1088 cm^{-1} attributed to the bending vibration of Ti–OH is shifted to a lower wavenumber (at 993 cm^{-1}) due to the creation of Ti–O–Si in the spectrum of APTES-TiO_2. The formation of the Ti–O–Si group was confirmed from the FTIR spectrum. Such linkage enables better interaction with the polymeric matrix as compared to the non-functionalized particles. It is expected that the enhanced filler-matrix adhesion would lead to less debonding of particles when stressed during sliding and hence less wear.

Density

The densities of the composites are given in **Table 3**. The density of the composite increased with an increase in TiO_2% since it is heavier (4.23 g/cc) than UHMWPE (0.93 g/cc). When comparing the densities of V_{2M} (0.952 g/cc), V_{2N} (0.967 g/cc), and F_{2N} (0.969 g/cc), which contained 2 wt.% Titania particles, it was observed that density was highest where functionalized NPs were used and lowest where untreated MPs were used.

Vickers Hardness

It can be observed from **Table 3** that:

- TiO_2, being a harder filler, increased the micro-hardness of the softer polymeric matrix.
- The hardness of composites increased significantly with increasing content of TiO_2 for MCs and NCs with functionalized particles (F-NCs), indicating good homogeneity of the filler dispersed in the composites. Improvement was highest for F-NCs, ≈60%.
- If the hardnesses of MCs, NCs, and F-NCs with the same amount of particles is compared, they showed the trend V_{2M} (6.967) < V_{2N} (8.14) < F_{2N} (8.20).

Void Contents

The void contents of the composites showed the following trends.

F-NCs

- Showed no void contents, indicating ideal composites.
- With increasing contents of MPs and NPs, void contents increased, though not proportionally.
- Void content was highest for MCs followed by NCs, and it was lowest for F-NCs, as follows: V_{2M} (3.3%) > V_{2N} (1.32%) > F_{2N} (0%)

Wettability Analysis of the Surfaces of Composites

Titania particles, being ceramic, have higher surface energy (72 dynes/cm) than the polymers, UHMWPE (30 dynes/cm) in this case (Travis Curtis, 2013; www.tstar.com, 2020). Hence, it was expected that the inclusion of NPs of Titania in UHMWPE would increase the surface energy of a composite. Their functionalization should do this to a still greater extent. Hence, surface energy or hydrophilicity was evaluated indirectly by wettability studies using a water drop. The UHMWPE showed an angle of around 91°, while those for V_{2N} and F_{2N} were 85° and 82°, respectively, indicating increased hydrophilicity.

Tribo-Properties of Composites

Adhesive Wear

Adhesive wear tests were conducted initially for 100 N, which resulted in non-measurable wear. Results on adhesive wear at 200 N (73 MPa) are shown in **Figure 5**. At 300 N, the composites failed at varying sliding durations, mostly due to melting of polymer.

Figure 5A1 shows the effect of inclusion of MPs, NPs, and F-NPs (all 2%) on adhesive wear of UHMWPE. V_0 (virgin UHMWPE) showed the lowest wear rate ($5 \times 10^{-15} m^3/Nm$). Inclusion of Titania particles (irrespective of size and functionalization) led to an increase in friction (**Figure 5A2**) and wear rate in spite of an increase in the hardness of all of the composites. This was mainly because of the irregular shape of both types of Titania paticles (MPs and NPs). Inclusion of particles of solid lubricants such as PTFE and graphite facilitates beneficial film transfer on the counterface, leading to a reduction in metal asperity-contacts and hence reducing friction and wear. Titania particles do not have a layered lattice structure, and hence, beneficial film formation was not expected. An increase in hardness does not ensure an increase in performance in adhesive wear. If the hard particles are spherical, they may act as load-bearing elements and convert area contact to more of a point contact, thereby reducing the probability of metallic asperities penetrating in the polymer composite. This may lead to performance improvement. In the present case, however, irregularly shaped particles with sharp edges posed the severe problem of third-body abrasion. These particles, especially MPs, were debonded easily during initial sliding because of their weaker bonding with the matrix. Once they appear in the debris, they start abrading both the parent surfaces, and adhesive wear is changed to three-body abrasive wear, showing higher friction and wear. MPs were so dominant in third-body

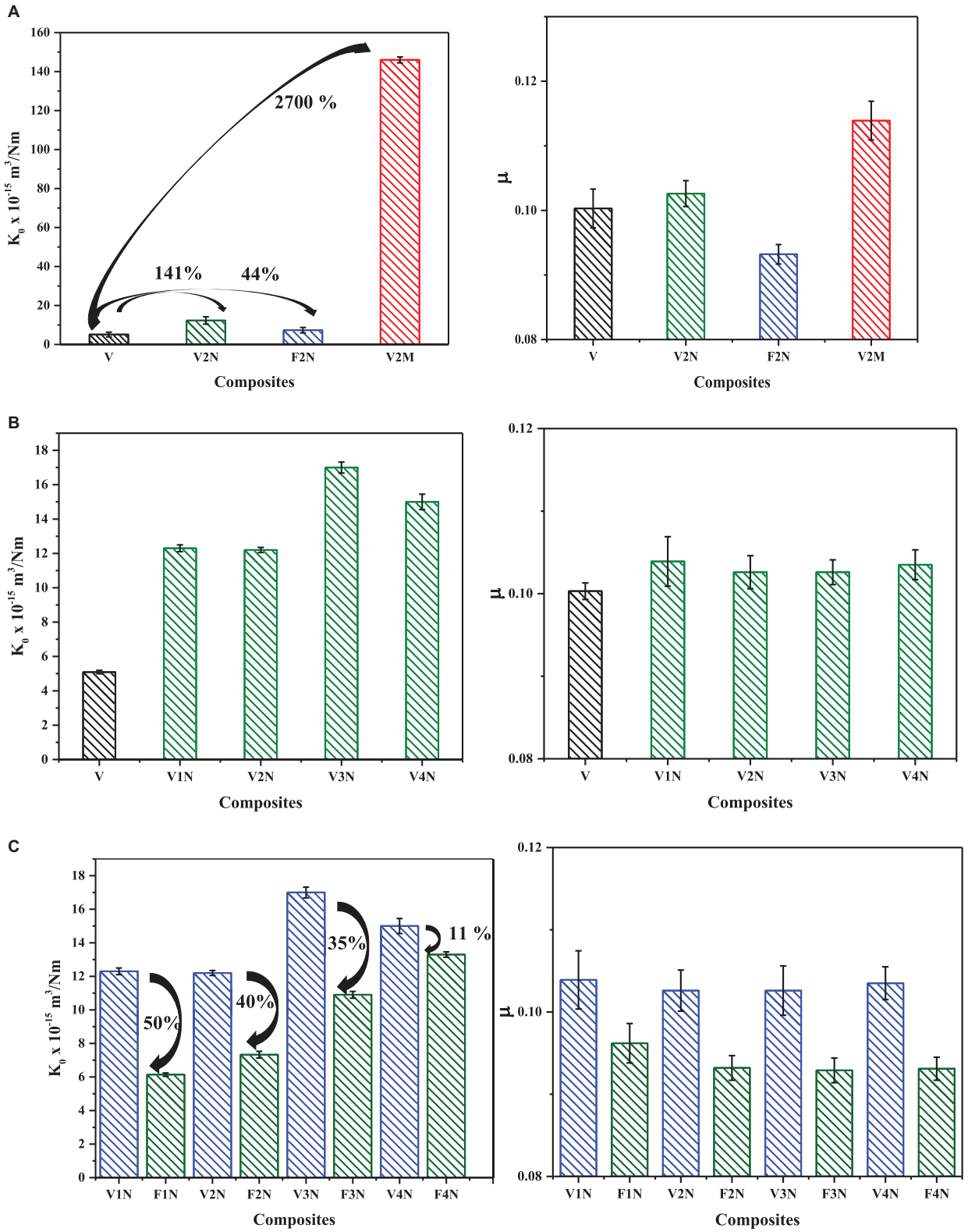

FIGURE 5 | Specific wear rate (K_0) **(a_1,b_1,c_1)** and μ **(a_2,b_2,c_2)** of composite disks against a ball (P – 73 MPa, speed – 0.014 m/s, sliding duration – 4 h). **(A)** Comparison of MC, NC, and F-NC (all with 2% particles) with UHMWPE; **(B)** Influence of increasing amount of NPs, and **(C)** benefits of functionalization of NPs.

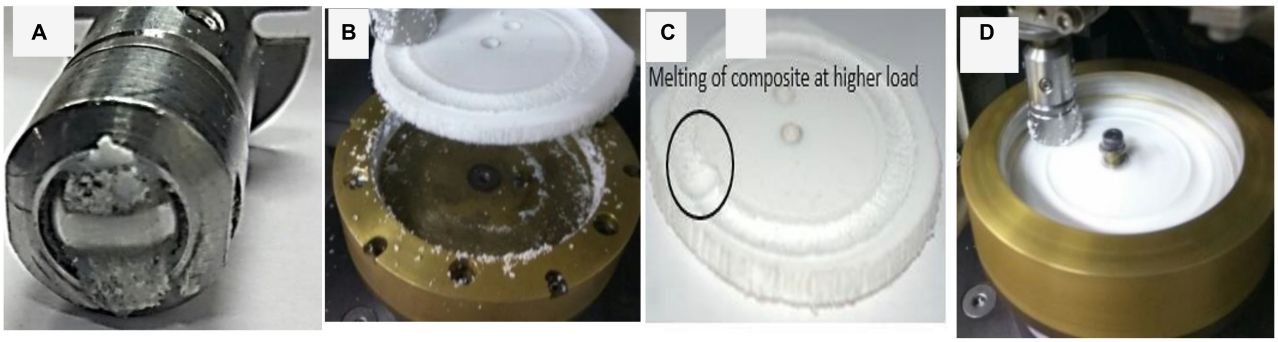

FIGURE 6 | Failed ball **(A)** against disks of a microcomposite **(B,C)** at 300 N and **(D)** disk of UHMWPE at 300 N.

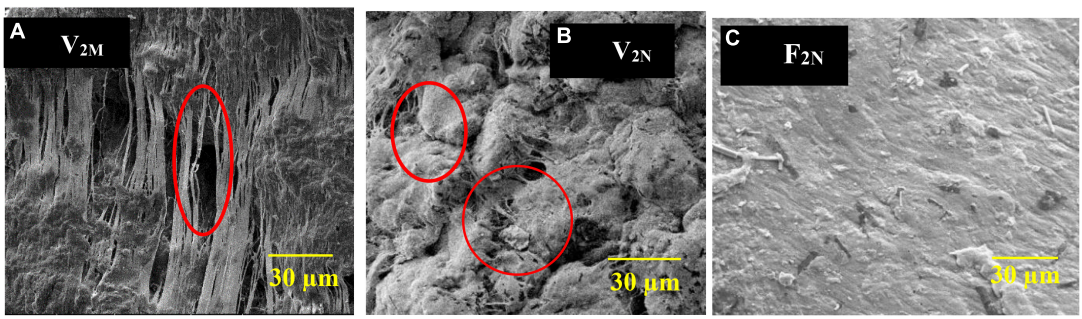

FIGURE 7 | Worn surfaces of composites disks **(A)** V_{2M}, **(B)** V_{2N}, and **(C)** F_{2N} tested at 200 N, 0.15 m/s.

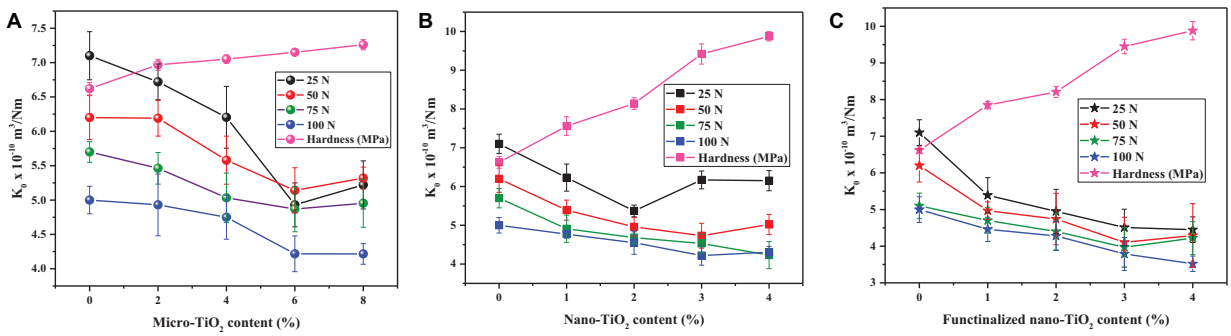

FIGURE 8 | Effect of contents of Titania particles on the abrasive wear of UHMWPE as a function of load for **(A)** microcomposites (MCs), **(B)** nanocomposites (NCs), and **(C)** functionalized nanocomposites (F-NCs).

abrasion that during interaction with the steel ball surface, μ was quite high, which led to an excessive increase in frictional torque and hence heat. The polymer disk, having low thermal conductivity (TC), could not dissipate this heat so efficiently, leading to the removal of softened matrix and debonded MPs, easily accounting for the very high wear of this MC (2700% higher than UHMWPE).

In the case of NPs and F-NPs, wear rates increased by 141 and 44% for V_{2N} and F_{2N}, respectively. The influence of NPs in composites on performance depends on their type (abrasive or solid lubricant), amount, size, shape, etc. Harder particles, if spherical or cylindrical, can act as ball/roller bearings, reducing friction and wear in adhesive wear mode, although not much is reported on the influence of the shape of NPs on the adhesive wear of composites (Jia et al., 2006; Shi et al., 2007). In the current case, harder particles were of irregular shape and hence deteriorated the tribo-performance of UHMWPE. For NPs, the digging out process was not so dominant since they had more interaction with the matrix because of their nano size. Hence, debris contained a smaller number of NPs, and third-body abrasion was not so prominent and detrimental. In the case of functionalized NPs, the process of digging out of particles was still more reduced because of stronger filler-matrix adhesion, and the extent of deterioration to the performance also decreased.

TABLE 4 | Average roughness of worn composite disks.

Composites	R_a(μm)	Composites	R_a(μm)	Composites	R_a(μm)
V	1.45	1.45	1.45	1.45	1.45
V_{1M}	1.75	V_{1N}	1.54	F_{1N}	1.53
V_{2M}	1.74	V_{2N}	1.76	F_{2N}	1.45
V_{3M}	1.89	V_{3N}	1.77	F_{3N}	1.57
V_{4M}	2.2	V_{4N}	1.84	F_{4N}	1.79

As seen in **Figure 5B1**, an effect whereby an increasing amount of NPs leads to increased friction and wear can be seen, although it is not strictly linear. **Figures 5C1,5C2** show how treatment of particles improved the performance of NCs.

Failed Surfaces and SEM Studies

Table 4 shows the average roughness (R_a) of the wear tracks of composites worn at 200 N. With increasing contents of particles, disk surface roughness increased in almost all composites, which is indirect evidence of third-body abrasion of the disk because of more particles being released in the debris. Interestingly, if R_a values are compared row-wise, they were highest for MPs followed by NPs and lowest for F-NPs, in general, indicating that the severity of third-body abrasion was at a maximum in the case of MPs and at a minimum for F-NPs.

Figures 6A,D show photographs of failed ball and disk surfaces of MC when slid under 300 N. The failure was characterized by excessive wear of the disk and adherence of the softened wear debris to the ball surfaces. It also shows localized melting of the wear track at a particular location (**Figure 6C**). An UHMWPE disk (**Figure 6D**) with excessive wear can also be seen.

SEM of Worn Surfaces of Disks

Although the experiments could run for 4 h, the surfaces show some marks of melting (**Figure 7A**) in the case of MC since frictional heat was very high. The shearing forces on the high-temperature surfaces elongated/fibrillated the UHMWPE. In the case of NC (**Figure 7B**), such marks are negligible (marked), and surface is very rough. In the case of F-NC (**Figure 7C**), fibrillation marks are not evident since the melting phenomenon was milder due to lower frictional heat. However, the entire surface of composite disc shows evidence of softening and then solidifying after the test.

Abrasive Wear

Incorporation of particles proved beneficial for UHMWPE in the case of abrasion resistance, as seen in **Figure 8** for MCs, NCs, and F-NCs (K_0 as a function of contents of Titania particles) and **Figure 9** in comparisons of MCs vs. NCs and NCs vs. F-NCs (K_0 as a function of load). It was observed that:

- K_0 was in the range of 3–7 × 10^{-10} m^3/Nm for the composites.
- With increase in load, K_0 decreased, which is in line with Lhymn's equation (Lhymn, 1987),

$$K_0 = K\frac{v_s}{EH\varepsilon\mu}V_c\frac{1}{F_N^{\delta}} \quad (10)$$

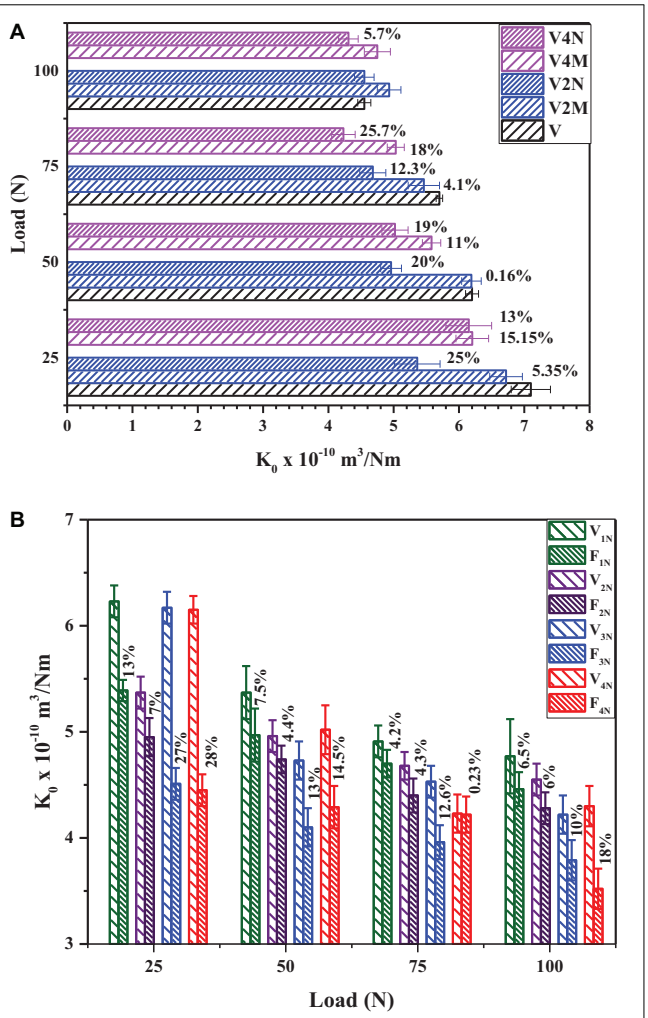

FIGURE 9 | Comparative abrasive wear performance at various loads for **(A)** nanocomposites (NCs) and microcomposites (MCs) (% indicates the% improvement in wear resistance as compared to neat UHMWPE) and **(B)** NCs and functionalized nanocomposites (F-NCs) (% indicates the% improvement in wear resistance as compared to non-functionalized NCs).

where K_0 is the specific wear rate, V_s is the sliding speed, E is the elastic modulus, H is the hardness, ε is the critical wear strain, μ is the friction coefficient, V_c is the crack growth velocity, and F_N is the normal load. At lower loads, variation was higher. It also shows that wear is inversely propotional to hardness.

- With increase in the amount of MCs (0–8 wt.%), K_0 was lowest for 6% followed by a slight rise for 8% (**Figure 8A**). The highest reduction (29%) in K_0 was for V_{6M} at 25 N.
- For NCs, the optimum contents for the lowest K_0 were in the range of 3%, barring 25 N, where it was 2% (**Figure 8B**), and the highest reduction in K_0 was for 2% (22%) at 25N.
- For F-NCs, the optimum contents for the lowest K_0 were in the range of 3%, barring 25 N, where it was 2% (**Figure 8C**), and the highest reduction in K_0 was for 2% (33%) at 25N.

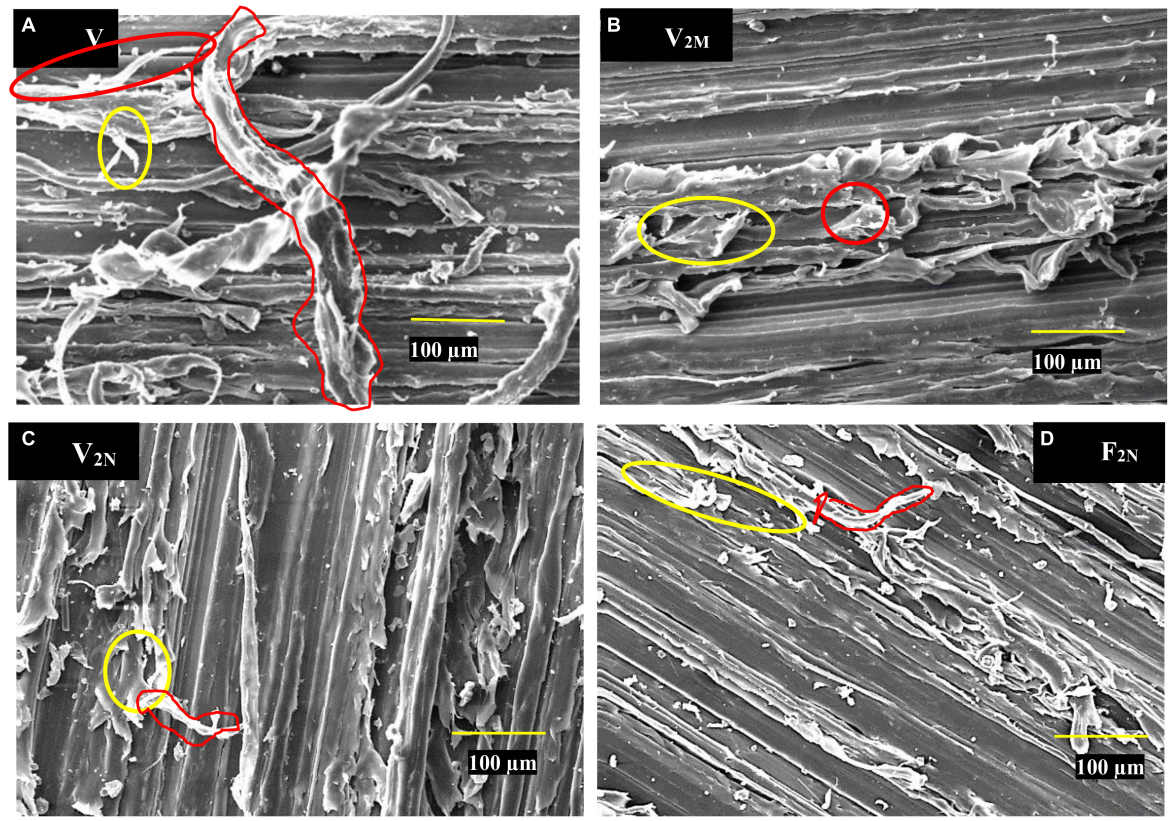

FIGURE 10 | Worn surfaces of composite pins abraded by *SiC* paper at 75 N, 25 mm/s for **(A)** V_0, **(B)** V_{2M}, **(C)** V_{2N}, and **(D)** F_{2N} (secondary micro-cutting indicated by yellow ellipses).

- In general, NCs exhibited superior performance to MCs (**Figure 9A**).

The reasons for wear resistance enhancement are explained in the section below on worn surface analysis.

Worn Surface Analysis by SEM

SEM micrographs of composite pins abraded by *SiC* paper at 75 N are shown in **Figures 10A–D**. The hardness of composites was in the order UHMWPE (6.621 MPa) < V_{2M} (6.968 MPa) < V_{2N} (8.14 MPa) < F_{2N} (8.21 MPa), and wear rate also followed the same order. In abrasive wear, micro-cutting and microplowing are the two major wear mechanisms. Micro-cutting, which is indicated by ribbon-shaped elongated debris and further fibrillation (secondary micro-cutting) due to abrasion by successive grits, and microplowing are the most prominent mechanisms in abrasion for ductile polymers like UHMWPE and PTFE (Hutchings, 1992). Indeed, microplowing occurs in both ductile and brittle polymers. It has a direct correlation with hardness: harder polymers are more resistant to microplowing. In the case of composites with hard fillers like Titania, an additional mechanism of digging out of particles during microplowing also plays an important role. Ease of digging out depends on the size and shape of particles and their bonding with the polymer. Rounded particles can be easily dug out while being abraded by the *SiC* grits, while irregularly shaped particles resist to a greater extent. After being dug out, the particles appear in wear debris. These then start damaging the *SiC* grits and their abrasivity. The higher the hardness, the higher is the damaging power, and the higher is the protection to the polymer composite from the grits during further abrasion.

As seen in Micrograph 10a, excessive micro-cutting and secondary micro-cutting were reponsible for the highest wear of UHMWPE. The depth of grooves due to microplowing is also highest, since UHMWPE has the lowest hardness. Moving from UHMWPE to V_{2M}, hardness increased, and both microplowing and micro-cutting were abruptly reduced. Drastically decreased ductility of the composite can be seen from the edges of ribbons (marked). The depth of grooves is also reduced, indicating reduced extents of both phenomena, supporting the lower wear of this MC.

For NC (**Figure 10C**) and then F-NC (**Figure 10D**), increased ductility (due to their being NCs) can be observed along with secondary micro-cutting. The microplowing is drastically reduced, especially for F-NC, where it is reduced to the extent that the surface topography appears to be quite smooth. This supports the lowest wear occurring in this composite.

Supplementary Appendix A elaborates on the difference in adhesive and abrasive wear and the reasons behind it.

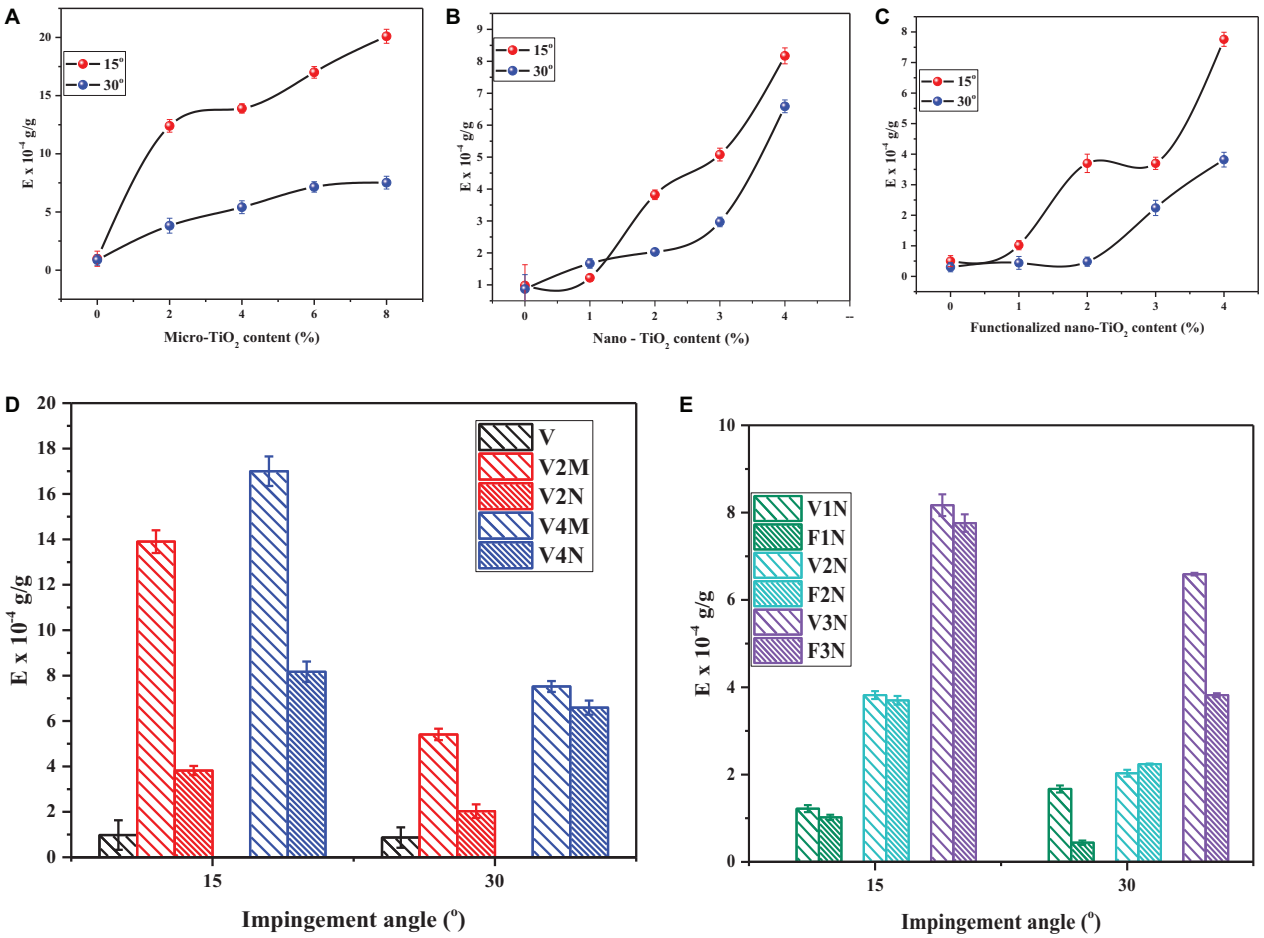

FIGURE 11 | Erosion as a function of amount of particles for two angles; **(A)** microcomposites (MCs), **(B)** nanocomposites (NCs), and **(C)** functionalized nanocomposites (F-NCs); comparative erosion performance for **(D)** MCs and NCs, and **(E)** NCs and F-NCs.

Erosive Wear

Erosive wear is a complex wear mode, and in case of particulate composites, wear resistance is always deteriorated, mainly due to the ease with which particles are detached and thrown off. The literature reports that in spite of increasing hardness, wear performance always decreases (Suh, 1986). An enhancement of performance has only been reported for Aramid and Zylon fabric reinforced composites (Sharma et al., 2019). **Figure 11** shows the erosion performance of composites eroded at two angles. In all cases, erosion of composites was higher at 15°, indicating super-ductile failure (Hutchings, 1992).

It was observed that the virgin UHMWPE was the best performer. Inclusion of Titania particles deteriorated the performance significantly in spite of an increase in hardness. The extent of deterioration increased with increase in Titania particle content, being at a maximum for MPs and a minimum for F-NPs. Erosion definitely depends on the hardness of the analyte material. In the case of composite, which is a heterogeneous material, however, hardness does not help. It depends on the ease with which particles are dislodged from the matrix during bombardment. NPs definitely lead to more homogeneity of the composite and have many-times superior particle–matrix adhesion because of the increased surface activity of NPs. It is not so easy to dislodge NPs, and hence wear of NCs was significantly less severe than that of MCs. Interestingly NC with 1% Titania showed quite similar behavior to UHMWPE. For functionalized NCs, adhesion was still stronger, and hence erosion performance was the best among all of the particulate composites. **Figures 11D,E** demonstrates this comparative behavior more clearly.

CONCLUSION

In this study, composites of UHMWPE and Titania were developed with three objectives, viz, to investigate the size effect (nano vs. micro), the amount effect, and the particle-functionalization effect.

It was worth pointing out that the testing conditions in this work were not in tune with testing for biomedical applications, although UHMWPE composites are being researched for the same. There is scope to extend this work in that direction. This

work is instead an indication of how abrasive wear resistance of UHMWPE can be increased by incorporating functionalized Titania NPs of irregular shape. The same theme may possibly work to enhance adhesive wear resistance if spherical NPs with functionalization could be used.

Based on the investigations on the three series of composites, the following conclusions are drawn.

- Functionalization of NPs led to increased adhesion with the matrix, as evident from the increased density (compactness) and lowering of contact angle (increased hydrophilicity).
- Inclusion of particles increased the hardness of composites. The higher the amount, the higher was the hardness. For composites with the same amount of particles (2%), functionalized nanocomposite (F-NC) showed the highest hardness, followed by NC, and then MC.
- Based on the abrasive wear studies, the optimum% of MPs for the highest improvement (20%) in wear resistance was 6%, while for nano-series, it was 3% for attaining a 28% improvement. Functionalized NPs proved most effective, and a 35% improvement in wear resistance was observed for 3 wt% of F-NPs. Increase in hardness was found to be the major reason for this, as it was responsible for reducing the severity of dominating wear mechanisms viz micro-cutting and microplowing significantly, as confirmed from the SEM studies.
- In the case of adhesive and erosive wear modes, however, the inclusion of particles led to a deterioration in performance, which depended on the size, amount, and functionalization of NPs. It was concluded that the increase in hardness did not help to increase the wear performance in these two wear modes. The irregular shape of MPs and NPs was the main controlling parameter. Including 2% MPs deteriorated the performance of UHMWPE excessively (2400%) in adhesive wear mode, while NPs reduced it by 140%. F-NCs were least detrimental (40% deterioration). Third-body abrasion appeared to be the dominating wear mechanism due to released particles from the composites accumulating as wear debris in adhesive wear mode. An increase in the roughness of worn surfaces supported this phenomenon.
- In the case of erosive wear, UHMWPE again proved best, followed by F-NCs and then NCs. MCs proved worst, and the higher the amount of particles, the more severe was the deterioration. It was concluded that the ease with which particles are dislodged from the composites during bombardment was the key factor controlling the erosion of composites. F-NCs proved best in this respect since particle–matrix bonding was the best. The composites showed failure in super-ductile mode by exhibiting the highest erosion at 15°.

The most important conclusions regarding the selection of particles to improve the hardness and wear resistance of UHMWPE are as follows.

The type, size, amount, shape, and filler–matrix adhesion are the most important aspects. Nano-sized particles worked best, and a content of around 3% proved optimum. Siloxane treatment proved very effective in improving all performance properties. However, the shape of particles controlled adhesive wear performance in an adverse way. For abrasive wear mode, it was appropriate.

DATA AVAILABILITY STATEMENT

The raw data supporting the conclusions of this article will be made available by the authors, without undue reservation.

AUTHOR CONTRIBUTIONS

MP conducted and repeated many experiments and performed the manuscript writing and data analysis. GP developed composites, conducted several experiments, and helped in data compilation along with figures and tables. JB performed to identifying and conceptualizing of the problem and supervision during implementation, analysis of the data, helped in writing the draft of the manuscript, and contributed extensively for the depiction of the ideas for the present. All authors contributed to the article and approved the submitted version.

ACKNOWLEDGMENTS

The authors are thankful to Mr. Bhaskaranand Bhatt (Research Scholar, Indian Institute of Technology Delhi) for providing help in SEM work.

SUPPLEMENTARY MATERIAL

The Supplementary Material for this article can be found online at: https://www.frontiersin.org/articles/10.3389/fmats.2020.00205/full#supplementary-material

REFERENCES

Coker, R. (2019). *Parx Plastics Granted Antimicrobial Vitamin e-blended UHWMPE patent*. Available online at: https://www.eppm.com/materials/parx-plastics-granted-antimicrobial-vitamin-e-blended-uhwmpe/ (accessed May 1, 2020).

Celebi Efe, G., Altinsoy, I., Türk, S., Bindal, C., and Ucisik, A. H. (2019). Effect of particle size on microstructural and mechanical properties of UHMWPE–TiO2 composites produced by gelation and crystallization method. *J. Appl. Polym. Sci.* 136, 15–18. doi: 10.1002/app.47402

Celebi Efe, G., Bindal, C., and Ucisik, A. H. (2017). Characterization of UHWPE-TiO2 composites produced by gelation/crystallization method. *Acta Phys. Pol. A* 132, 767–769. doi: 10.12693/APhysPolA.132.767

Chahar, B. S., and Pun, A. K. (2018). Erosion wear of ductile materials: a review. *ELK Asia Pacific J.* ISBN: 978-81-930411-8-5.

Chang, B. P., Akil, H. M., and Nasir, R. M. (2013). Mechanical and tribological properties of zeolite-reinforced UHMWPE composite for implant application. *Proc. Eng.* 68, 88–94. doi: 10.1016/j.proeng.2013.12.152

Chang, B. P., Akil, H. M., Nasir, R. M., and Nurdijati, S. (2011). Mechanical and antibacterial properties of treated and untreated zinc oxide filled UHMWPE composites. *J. Thermoplast. Compos. Mater.* 24, 653–667. doi: 10.1177/0892705711399848

Chukov, D. I., Stepashkin, A. A., Gorshenkov, M. V., Tcherdyntsev, V. V., and Kaloshkin, S. D. (2014). Surface modification of carbon fibers and its effect on the fiber-matrix interaction of UHMWPE based composites. *J. Alloys Compd.* 586, S459–S463. doi: 10.1016/j.jallcom.2012.11.048

Duan, W., Wu, M., Han, J., and Ni, Z. (2020). Research into the thermal stability and mechanical properties of vitamin e diffusion modified irradiation cross-linked graphene oxide/ultra-high molecular weight polyethylene composites. *RSC Adv.* 10, 4175–4188. doi: 10.1039/c9ra09893c

Gao, Y., Feng, X., Liu, J., Fu, H., Li, S., and He, C. (2019). Design and ballistic penetration of "SiC/Ti6Al4V/UHMWPE" composite armor. *IOP Conf. Ser. Mater. Sci. Eng.* 563:042043. doi: 10.1088/1757-899X/563/4/042043

Ge, S., Wang, S., and Huang, X. (2009). Increasing the wear resistance of UHMWPE acetabular cups by adding natural biocompatible particles. *Wear* 267, 770–776. doi: 10.1016/j.wear.2009.01.057

Gopanna, A., Rajan, K. P., Thomas, S. P., and Chavali, M. (2019). *Polyethylene and Polypropylene Matrix Composites for Biomedical Applications*. Amsterdam: Elsevier Inc, doi: 10.1016/B978-0-12-816874-5.00006-2

Gutwein, L. G., and Webster, T. J. (2004). Increased viable osteoblast density in the presence of nanophase compared to conventional alumina and titania particles. *Biomaterials* 25, 4175–4183. doi: 10.1016/j.biomaterials.2003.10.090

Hashimoto, M., Takadama, H., Mizuno, M., Yasutomi, Y., and Kokubo, T. (2003). Titanium dioxide/ultra high molecular weight polyethylene composite for bone-repairing applications: preparation and Biocompatibility. *Key Eng. Mater.* 242, 415–418. doi: 10.4028/www.scientific.net/KEM.240-242.415

Holland, M., Fleming, L., Walton, K., Cerquiglini, A., Hothi, H., Hart, A., et al. (2018). Characterisation of wear areas on UHMWPE total knee replacement prostheses through study of their areal surface topographical parameters. *Surf. Topogr. Metrol. Prop.* 6:034006. doi: 10.1088/2051-672X/aac071

Holzwarth, U., and Gibson, N. (2011). The Scherrer equation versus the "Debye-Scherrer equation,". *Nat. Nanotechnol.* 6:534. doi: 10.1038/nnano.2011.145

Hu, J., Gao, Q., Xu, L., Zhang, M., Xing, Z., Guo, X., et al. (2016). Significant improvement in thermal and UV resistances of UHMWPE fabric through in situ formation of polysiloxane-TiO_2 hybrid layers. *ACS Appl. Mater. Interf.* 8, doi: 10.1021/acsami.6b04914

Hutchings, I. M. (1992). *Tribology: Friction and Wear of Engineering Materials*. Oxford: Butterworth-Heinemann.

Jia, Q. M., Zheng, M., Xu, C. Z., and Chen, H. X. (2006). The mechanical properties and tribological behavior of epoxy resin composites modified by different shape nanofillers. *Polym. Adv. Technol.* 17, 168–173. doi: 10.1002/pat.710

Kandeva, M., Kamburov, V., Nikolov, K., and Dimitrov, L. (2018). Abrasive wear of Ultra-High-Molecular-Weight Polyethylene (UHMWPE) modified with Carbon Nanotubes (CNTs). *Tribol. J. Bultrib* 7, doi: 10.13140/RG.2.2.28527.28327

Kumar, A., Bijwe, J., and Sharma, S. (2017). Hard metal nitrides: role in enhancing the abrasive wear resistance of UHMWPE. *Wear* 378–379, 35–42. doi: 10.1016/j.wear.2017.02.010

Lee, L. H. (1985). *Polymer Wear and Its Control*. Washington, DC: American Chemical Society. doi: 10.1016/0142-9612(86)90076-1

Lei, Y., Guo, J. L., and Zhang, Y. X. (2010). Tribological behaviour of nano-TiO_2 filled ultra high molecular weight polyethylene composites. *Polym. Mater. Sci. Eng.* 26, 48–51.

Lhymn, C. (1987). Effect of normal load on the specific wear rate of fibrous composites. *Wear* 120, 1–27. doi: 10.1016/0043-1648(87)90130-X

Mallakpour, S., and Nikkhoo, E. (2013). Production and characterization of nanocomposites based on poly(amide-imide) containing 4,4′-methylenebis(3-chloro-2,6- diethylaniline) using nano-TiO_2 surface-coupled by 3-aminopropyltriethoxysilane. *Prog. Org. Coatings.* 76, 231–237. doi: 10.1016/j.porgcoat.2012.09.022

Ortiz-Hernández, R., Ulloa-Castillo, N. A., Diabb-Zavala, J. M., La Vega, A. E. D., Islas-Urbano, J., Villela-Castrejón, J., et al. (2019). Advances in the processing of UHMWPE-TiO2 to manufacture medical prostheses via SPIF. *Polymers* 11:2022. doi: 10.3390/polym11122022

Sabetrasekh, R., Tiainen, H., Lyngstadaas, S. P., Reseland, J., and Haugen, H. (2011). A novel ultra-porous titanium dioxide ceramic with excellent biocompatibility. *J. Biomater. Appl.* 25, 559–580. doi: 10.1177/0885328209354925

Salari, M., Mohseni Taromsari, S., Bagheri, R., and Faghihi Sani, M. A. (2019). Improved wear, mechanical, and biological behavior of UHMWPE-HAp-zirconia hybrid nanocomposites with a prospective application in total hip joint replacement. *J. Mater. Sci.* 54, 4259–4276. doi: 10.1007/s10853-018-3146-y

Saravanan, I., and Devaraju, A. (2019). Wear mechanism of UHMWPE polymer composites for bio medical applications. *Mater. Res. Express* 6, 0–11. doi: 10.1088/2053-1591/ab3ed9

Senatov, F., Amanbek, G., Orlova, P., Bartov, M., Grunina, T., Kolesnikov, E., et al. (2020). Biomimetic UHMWPE/HA scaffolds with rhBMP-2 and erythropoietin for reconstructive surgery. *Mater. Sci. Eng. C* 111:110750. doi: 10.1016/j.msec.2020.110750

Senatov, F. S., Gorshenkov, M. V., Kaloshkin, S. D., Tcherdyntsev, V. V., Anisimova, N. Y., Kopylov, A. N., et al. (2014). Biocompatible polymer composites based on ultrahigh molecular weight polyethylene perspective for cartilage defects replacement. *J. Alloys Compd.* 586, S544–S547. doi: 10.1016/j.jallcom.2012.10.014

Sharma, S., Bijwe, J., and Panier, S. (2016). Assessment of potential of nano and micro-sized boron carbide particles to enhance the abrasive wear resistance of UHMWPE. *Compos. Part B Eng.* 99, 312–320. doi: 10.1016/J.COMPOSITESB.2016.06.003

Sharma, S., Bijwe, J., and Panier, S. (2019). Exploration of potential of Zylon and Aramid fibers to enhance the abrasive wear performance of polymers. *Wear* 422–423, 180–190. doi: 10.1016/j.wear.2019.01.068

Sharma, S., Bijwe, J., Panier, S., and Sharma, M. (2015). Abrasive wear performance of SiC-UHMWPE nanocomposites - Influence of amount and size. *Wear* 332–333, 863–871. doi: 10.1016/j.wear.2015.01.012

Shi, Y. J., Feng, X., Wang, H. Y., Liu, C., and Lu, X. H. (2007). Effects of filler crystal structure and shape on the tribological properties of PTFE composites. *Tribology Int.* 40, 1195–1203.

Suh, N. P. (1986). *Tribophysics, First Edition*. Upper Saddle River, NJ: Prentice Hall.

Travis Curtis (2013). *Surface Characterization of an Organized Titanium Dioxide Layer*. Master's Thesis, University of Arizona, Tucson. doi: 10.1017/CBO9781107415324.004

Ukaji, E., Furusawa, T., Sato, M., and Suzuki, N. (2007). The effect of surface modification with silane coupling agent on suppressing the photo-catalytic activity of fine TiO_2 particles as inorganic UV filter. *Appl. Surf. Sci.* 254, 563–569. doi: 10.1016/j.apsusc.2007.06.061

Wang, Q., Zhang, D., and Ge, S. (2007). Biotribological behaviour of ultra-high molecular weight polyethylene composites containing Ti in a hip joint simulator. *Proc. Inst. Mech. Eng. Part J: J. Eng. Tribol.* 221, 307–313. doi: 10.1243/13506501JET232

www.tstar.com (2020). Available online at: https://www.tstar.com/blog/bid/33845/surface-energy-of-plastics (accessed March 25, 2020).

Xu, S., and Tangpong, X. W. (2013). Review: tribological behavior of polyethylene-based nanocomposites. *J. Mater. Sci.* 48, 578–597. doi: 10.1007/s10853-012-6844-x

You, Y. L., Li, D. X., Si, G. J., and Deng, X. (2014). Investigation of the influence of solid lubricants on the tribological properties of polyamide 6 nanocomposite. *Wear* 311, 57–64. doi: 10.1016/j.wear.2013.12.018

Yu, W. W., Shi, J. G., Wang, L., Liu, Y. L., and Chen, X. X. (2017). Structure and mechanical properties of TiO_2/UHMWPE nanocomposite monofilaments. *MATEC Web. Conf.* 128, 2–4. doi: 10.1051/matecconf/201712803007

Conflict of Interest: The authors declare that the research was conducted in the absence of any commercial or financial relationships that could be construed as a potential conflict of interest.